https://doi.org/10.5194/egusphere-2026-1742
Preprint. Discussion started: 11 May 2026

Inefficient Consumption of Natural Gas Drives Methane Emissions from a Megacity

Yuwei Zhao[1,2], Andrew Hallward-Driemeier[1,2], Luke D. Schiferl[2], Trey Maddaleno[3], Michael P. Vermeuel[4], Dylan B. Millet[3], Delphine Farmer[5], and Róisín Commane[1,2]

[1]Department of Earth and Environmental Sciences, Columbia University, New York, NY 10027, USA
[2]Lamont-Doherty Earth Observatory, Columbia University, Palisades, NY 10964, USA
[3]Department of Soil, Water, and Climate, University of Minnesota, St. Paul, MN 55108, USA
[4]Department of Earth, Atmospheric, and Planetary Sciences, Purdue University, West Lafayette, IN, 47907, USA
[5]Department of Chemistry, Colorado State University, Fort Collins, CO 80523, USA

Correspondence: Yuwei Zhao (yz4343@columbia.edu)

Abstract. Reducing methane emissions offers a significant near-term opportunity for climate mitigation if the dominant sources are effectively targeted. Natural gas is a large and manageable methane source. Despite extensive pipeline upgrades in cities, methane reductions remain far smaller than expected, suggesting missing emission pathways. Using long-term tower observations in a U.S. megacity, we found a strong seasonal cycle in methane emissions peaking during the winter heating and summer cooling seasons. Natural gas methane emissions dominated both seasons and were strongly correlated with consumption, yielding a loss rate of 1.7±0.6%, equivalent to about $300 M USD/yr of unused natural gas. Incomplete combustion was the primary natural gas signal observed, indicating future mitigation planning should prioritize inefficient natural gas consumption.

1 Introduction

Reducing methane (CH_4) emissions has become a goal of many global agreements (e.g. the Global Methane Pledge (Global Methane Pledge, 2021)) as a means to reduce climate warming in the short-term (Shindell et al., 2021). Atmospheric methane is a strong greenhouse gas with over 80 times the global warming potential of carbon dioxide (CO_2) over 20 years(Forster et al., 2021), and a relatively short atmospheric lifetime of 9.7 ± 1.1 years (Naik et al., 2021). Most programs use existing bottom-up methane emission estimates (also known as emission inventories) to decide where to focus their resources but not all processes are included in these estimates. Observation-based studies have indicated that urban methane emissions are often much larger than current bottom-up methane emission estimates (Pitt et al., 2022; Plant et al., 2019; Huang et al., 2019; Sargent et al., 2021; McKain et al., 2015). Additionally, many methane mitigation studies have focused on fossil fuel production and distribution (United Nations Environment Programme, 2025a, b), but few have considered end-use methane emissions (Saint-Vincent and Pekney, 2020; Merrin and Francisco, 2019; Fischer et al., 2018; Lebel et al., 2022). The distinction between pre-meter and post-meter methane emission has implications for what party is responsible for methane mitigation and how it should be implemented: Pre-meter leaks are addressed by the energy company providing the natural gas, while post-meter release is the responsibility of individual end-users. Identifying whether the methane is from a natural gas leak or has been

https://doi.org/10.5194/egusphere-2026-1742
Preprint. Discussion started: 11 May 2026

partially burned in an appliance also changes the steps required to reduce these methane emissions. By not considering end-use methane emissions, especially in cities, we may miss opportunities to greatly reduce methane emissions.

The New York City Metropolitan Area (NYCMA) has been identified as one of the world's top 100 largest persistent sources of methane (Vanselow et al., 2024) and is the largest area source of methane in the Northeastern United States (U.S.)(Plant et al., 2019; Floerchinger et al., 2021; Mueller et al., 2025). Long-term tower(Schiferl et al., 2025; Mueller et al., 2025), airborne (Plant et al., 2019; Floerchinger et al., 2021; Pitt et al., 2022, 2024), and satellite-based (Plant et al., 2022; Nesser et al., 2024) studies have estimated 2-5 times more methane emissions from NYCMA than can be explained by the existing national (Maasakkers et al., 2016) and global (Crippa et al., 2020) bottom-up estimates. However, the specific emission processes responsible for this missing methane remain poorly understood.

Like many cities, the largest methane sources in NYCMA include an aging natural gas system (natural gas transmission, distribution, and end-use; also known as thermogenic methane) and a waste management sector (landfills and wastewater treatment plants; also known as microbial methane)(Pitt et al., 2024; Maasakkers et al., 2023; Crippa et al., 2024). Natural gas is used for electricity generation all year round. The NYCMA mandates that residential buildings provide heating in heating season from October to May (New York City Housing Authority, 2025), with boilers and furnaces in buildings consuming more natural gas when temperatures are coldest. Some large buildings also use natural gas coupled with heat exchangers for cooling during the non-heating season. The natural-gas-powered cooling units are common in urban areas globally too. Eddy covariance measurements in Sakai, Japan shows a strong temperature dependence in methane emissions, with peaks in both winter and summer, and suggest that peaked summertime emissions can be driven by natural gas-powered cooling units with lower combustion efficiency than heating units(Ueyama et al., 2025).

Natural gas contains methane and other hydrocarbons, such as ethane. Comparing the observed atmospheric ethane-to-methane ratio with that reported for the natural gas system allows attribution of the thermogenic fraction of methane emission in urban areas(Karion et al., 2015; Ren et al., 2018; Yacovitch et al., 2017; Peischl et al., 2018; Mielke-Maday et al., 2019; Menoud et al., 2022; Lopez et al., 2017; Maazallahi et al., 2020; Schwietzke et al., 2025; Simpson et al., 2012; Lamb et al., 2016). Using these methods, previous studies consistently pointed to natural gas as a major contributor to methane emissions from the NYCMA (Pitt et al., 2022, 2024; Plant et al., 2019; Floerchinger et al., 2021), with some estimates up to 10 times larger than national methane inventory emissions (Plant et al., 2019). One high-resolution methane inventory for the NYCMA estimated about 1.3 times higher methane emissions than the national inventories, but airborne methane observations indicated that this inventory still underestimated thermogenic emissions by a factor of 2.3 (Pitt et al., 2024).

Some studies have made steps towards resolving which specific natural gas processes are driving these missing emissions. Schiferl et al. (2025) suggested that stationary incomplete combustion is a dominant and underappreciated winter source of methane over the NYCMA, based on multi-year wintertime observations of carbon monoxide (CO) and methane (Schiferl et al., 2025). But the absence of concurrent ethane measurements in Schiferl et al. (2025) limited their ability to identify if the methane was thermogenic in origin and to determine the specific thermogenic drivers(Schiferl et al., 2025). Sargent et al., (2021) and Mckain et al. (2014) observed larger than expected methane emissions in Boston that were correlated with natural gas consumption. But they were unable to distinguish between natural gas transmission (pre-meter) or end-use (post-meter

https://doi.org/10.5194/egusphere-2026-1742
Preprint. Discussion started: 11 May 2026

or post-appliance combustion)(Sargent et al., 2021; McKain et al., 2015). Currently, the lack of process-level attribution of methane emissions limits our ability to develop effective methane mitigation policies and reduce urban methane emissions.

In this study, we present the first monthly source attribution of thermogenic methane emissions from pre- and post-meter natural gas sectors in the largest megacity in the USA by analyzing correlations between coincident 1 Hz measurements of methane, ethane, and carbon monoxide (CO). We also calculated observation-informed monthly methane emissions from January 2023 to December 2024 using long-term observations. Our findings provide insights into seasonal methane emissions from the NYCMA and reveal the total natural gas methane loss rate and seasonal thermogenic methane emission fractions for this urban area.

2 Methodology

In this study, we coupled a Lagrangian atmospheric transport model with global, national, and regional bottom-up methane estimates and compared the results with long-term hourly tower-based methane observations to quantify monthly NYCMA methane emissions from January 2023 to December 2024. We used trace gas correlations of methane, ethane, and CO from complementary measurement campaigns to attribute methane sources from May to August 2023 and in February 2024. We also compared the observation-informed monthly methane emissions with the borough-level natural gas deliveries to quantify the total natural gas loss rate from 2023 to 2024.

2.1 Long-term Tower Observations

The Mineola tower (40.7495°N, 73.6384°W) is a long-term National Institute of Standards and Technology (NIST) observatory located east of the NYC urban core, and it samples the integrated outflow from Manhattan and western Long Island during westerly winds (Figure 1). NIST greenhouse gas measurements at the Mineola Tower are designated MNY in Karion et al. (2023)(Karion et al., 2023a). MNY measures dry mole fraction of methane (CH_4, parts-per-billion, ppb, equivalent to nmol mol^{-1}) and carbon dioxide (CO_2, parts-per-million, equivalent to μmol mol^{-1}) with a calibrated Picarro G2301 operated since 2015 by Earth Networks under contract to NIST. We used the hourly MNY CH_4 sampled at 62 m AGL (above ground level) to estimate monthly methane emission rates across NYCMA from January 2023 to December 2024. We excluded October 2023 as there were only eight days of data that month. For regional methane background calculations, we used methane dry mole fractions from two other NIST sites (Stockholm, New Jersey: SNJ, and Hamden, Connecticut: HCT) and from the Lamont-Doherty Earth Observatory (LDEO) tower operated by the Commane group for the University of Rochester (Figure 1). The instruments at all sites are calibrated to the National Oceanic and Atmospheric Administration (NOAA) Global Monitoring Laboratory (GML), and are traceable to the World Meteorological Organization (WMO) scale for methane (WMO X2004A), CO_2 (WMO X2019) scale for consistency, with uncertainty archived at an hourly time resolution(Karion et al., 2023a; Verhulst et al., 2017; Welp et al., 2013; Karion et al., 2020). Detailed information about LDEO methane measurements can be found in Section S1. Hourly NIST-MNY methane time series from January 2023 to December 2024 is shown in Figure 2.

https://doi.org/10.5194/egusphere-2026-1742
Preprint. Discussion started: 11 May 2026

2.2 Targeted Field Campaigns

We used high-frequency atmospheric composition data from two intensive measurement campaigns to inform our analysis: the Fluxes of Reactive Organic Gases in New York (FROG-NY) campaign from May 19^{th} to August 10^{th} 2023, and the Fluxes of Reactive Organic Gases Seasonal Intercomparison of Chemistry, Lifetimes, and Emissions (FROGSICLE) campaign in February 2024. Dry mole fractions of methane (ppb), ethane (C_2H_6, ppb), carbon monoxide (CO, ppb), nitrous oxide (N_2O ppb), and CO_2 (ppm) were measured at the Mineola Tower at 60 m AGL using an Aerodyne SuperDUAL spectrometer(Commane et al., 2023) (Figure 2). We sampled from 60 m AGL in discrete 15-minute windows (e.g., 12:00–12:15 and 12:30–12:45, etc.) from May 19^{th} to July 21^{st}, 2023 and in 5-minute windows from July 21^{st} to August 10^{th}, 2023, and in 15-minute windows during February 2024. Trace gas dry mole fractions were calibrated to standards provided by the Central Calibration Laboratory (CCL) at the NOAA GML, and are traceable to the WMO scale for methane (WMO X2004A), CO (WMO X2014A), CO_2 (WMO X2019); and an internal CCL scale for ethane (C_2H_6-2012) and N_2O (NOAA-2006A) (detailed calibration informations can be found in supporting information Section S1).

Observations impacted by transported smoke during the 2023 summer Quebec wildfire events and by non-local clean marine air mass intrusion were excluded from the city-scale methane source attribution analysis (see details in Supporting Information Section S2).

2.3 Street-Level Observations

To complement our tower-based observations, we conducted street-level sampling of 1 Hz methane, ethane, CO, and N_2O dry mole fractions around the Mineola tower using the New York Atmospheric Composition and Air Quality (NYAAQ) Mobile Laboratory on August 16^{th}, 2023. More details are described in Section S3 and Figure S2. Trace gas correlations were used to characterize methane sources in the area around the tower.

2.4 Calculation of the Background

To accurately constrain the regional methane emission from NYCMA, it is critical to account for methane transported into the study domain from other regions, which we refer to as the methane *background*. The observed methane enhancements (ΔCH_4, ppb) were calculated as the difference between the observed and background methane (Eqn 1):

$$\Delta CH_4 = \text{Observed } CH_4 - \text{Background } CH_4 \quad (1)$$

We calculated methane backgrounds separately for the NIST-MNY and campaign-based trace gas measurements from the SuperDUAL. For NIST-MNY, methane background was derived from hourly dry mole fractions measured at the rural sites (Stockholm, Hamden, and LDEO, locations shown in Table S1). At each rural site, the upper 10^{th} percentile of the methane dry mole fractions from January 2023 to December 2024 was excluded to remove any local influences. For each hour, 1,000 bootstrap resamples with replacement were drawn per site over a centered 240-h moving window, conditional on at least 50% data availability. The mean methane background was calculated as the average across the total 3000 bootstrap resamples at

https://doi.org/10.5194/egusphere-2026-1742
Preprint. Discussion started: 11 May 2026

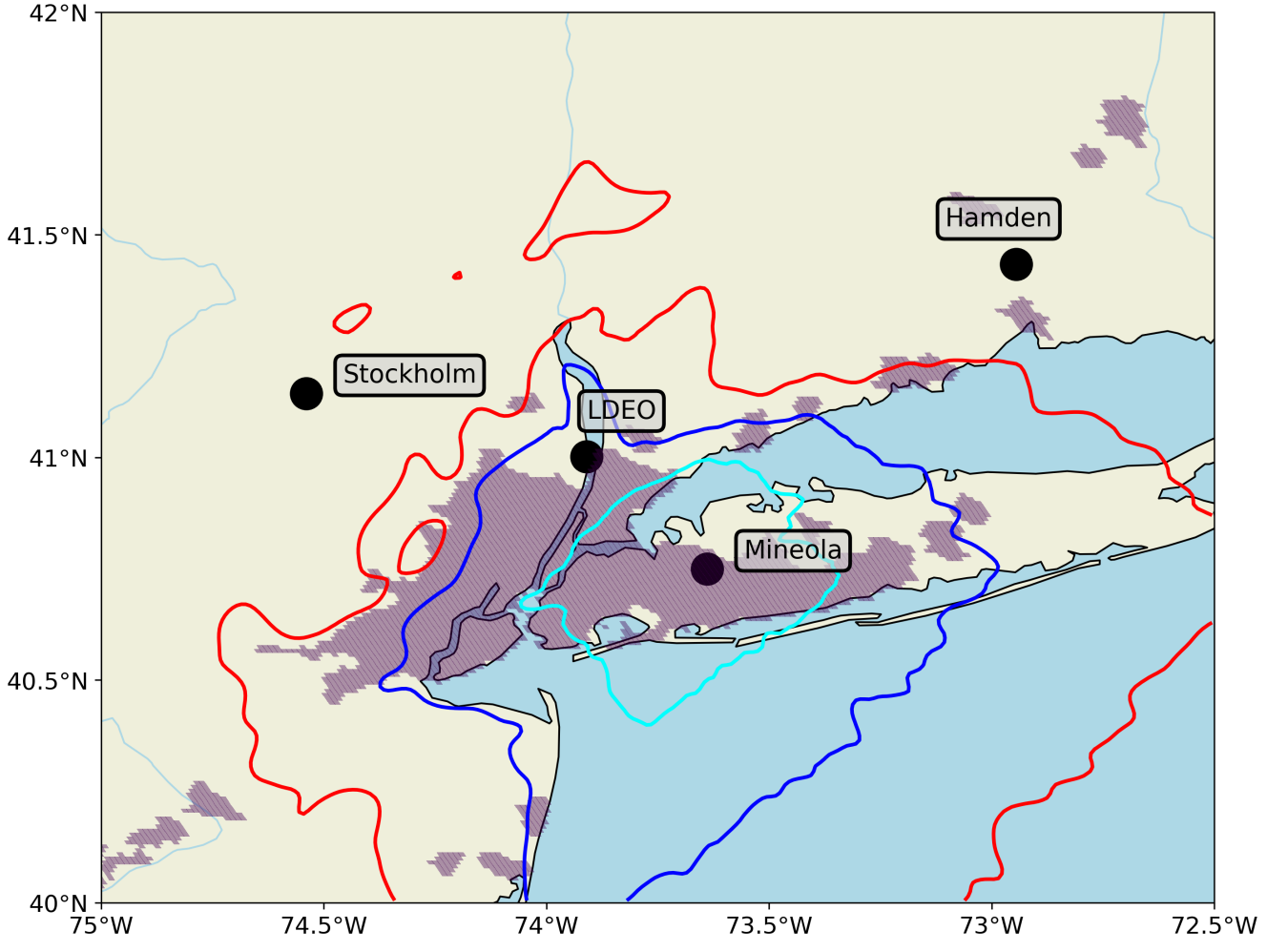

Figure 1. Map of in-situ observation towers within the New York City Metropolitan Area domain (NYCMA, longitude: 75.00°W to 72.50°W, latitude: 40.00°N to 42.00°N) used in this study. Urban areas are highlighted in purple based on the Global Human Settlement Layer(Schiavina et al., 2023). The solid contours indicate 50% (cyan), 75% (blue), and 90% (red) surface influence footprints for the NIST-MNY Mineola Tower (62 m AGL inlet, black circle) from January 2023 to December 2024. Black circles indicate tower observation sites at HCT, SNJ, and LDEO, which serve as rural background locations for long-term methane measurements in this study.

https://doi.org/10.5194/egusphere-2026-1742
Preprint. Discussion started: 11 May 2026

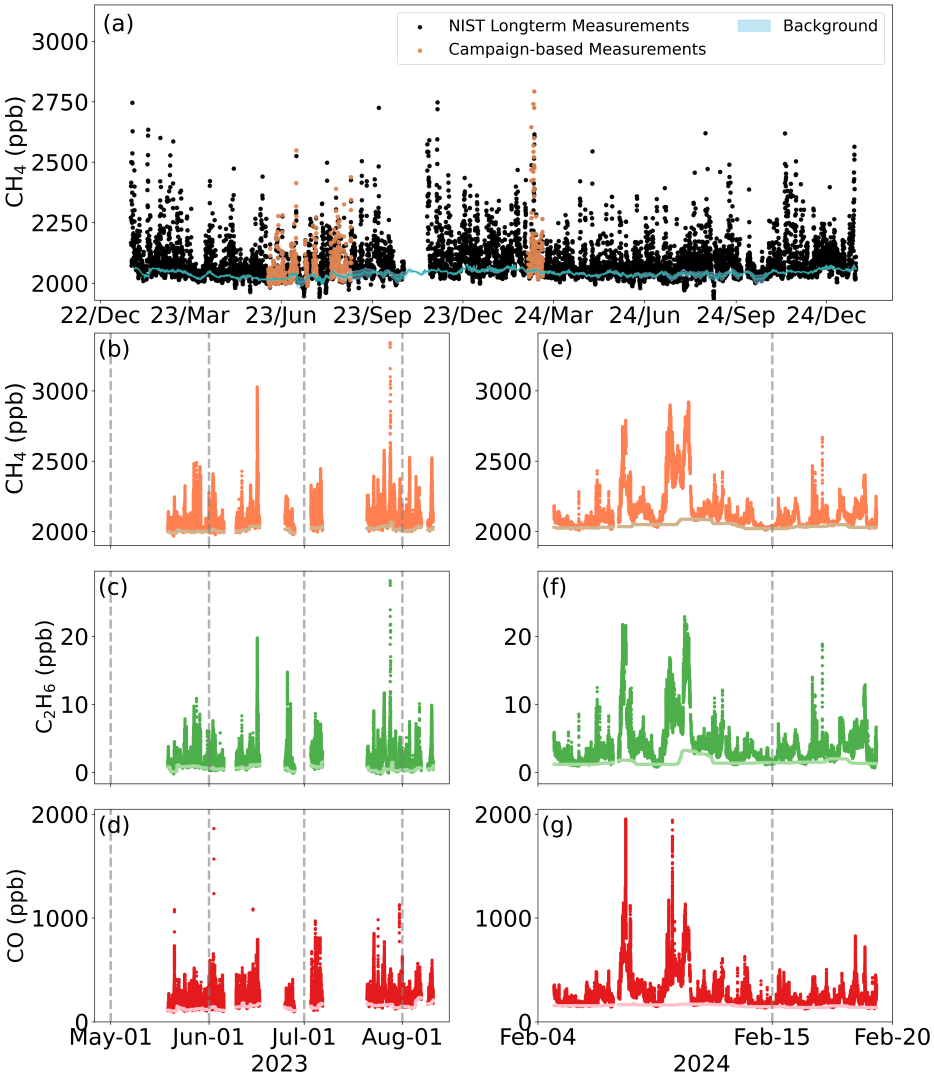

Figure 2. (a) Time series of hourly methane dry mole fraction measured at Mineola Tower. Black circles represent long-term NIST-MNY observations at 62 m AGL from January 2023 to December 2024, orange circles denote hourly campaign-based measurements of methane sampled from the Mineola Tower at 60 m AGL from May 19^{th} to August 10^{th}, 2023 and February 4^{th} to February 19^{th}, 2024. The mean (blue line) and variability (blue shading) of the NIST-MNY background methane dry mole fractions, calculated using the method described in the Calculation of the Background Section2.4, are also shown. (b), (c), (d) present time series of 1 Hz methane, ethane, and CO sampled from the Mineola Tower at 60 m (FROG-NY multi-trace gas measurements), respectively, from May 19^{th} to August 10^{th}, 2023, with corresponding 1 Hz background shown as light color in each subplot. (e), (f), (g) present time series of 1 Hz methane, ethane, and CO sampled from the Mineola Tower at 60 m (FROG-NY multi-trace gas measurements), respectively, from February 4^{th} to February 19^{th} 2024 (FROGSICLE multi-trace gas measurements), with corresponding 1 Hz background shown as light color in each subplot.

https://doi.org/10.5194/egusphere-2026-1742
Preprint. Discussion started: 11 May 2026

the three rural sites. The 25 and 75 percent confidence intervals (CI) of the bootstrap distribution were incorporated into the methane emission quantification uncertainty analysis. Variability of the background was relatively low in winter and spring (from 6–14 ppb in 2023 and 2024) but increased into summer months (6–30 ppb in 2023, and 13–24 ppb in 2024) (Figure S3).

There were no measurements of ethane or CO at other rural sites. For consistency, we calculated the trace gas background for 1 Hz campaign-based measurement SuperDUAL measurements as the lowest fifth percentile of the 1 Hz dry mole fractions over a centered 48-h running window for methane, ethane, and CO. Similar methods have been widely applied in other studies focusing on methane emission quantification (Sargent et al., 2021; McKain et al., 2015; Schiferl et al., 2024). All trace gas enhancements from the SuperDUAL (ΔCH_4, ΔC_2H_6, ΔCO) were calculated using Eqn 1, timeseries of multi-trace gas backgrounds are shown in Figure 2.

2.5 Source Attribution Analysis

Correlations between methane and co-emitted trace gases can be used to attribute likely methane emissions from different sources in a given air mass. Ethane is co-emitted from natural gas (thermogenic) sources: during natural gas extraction, processing, distribution, and end-use, but ethane is not emitted from microbial methane sources such as landfills, wastewater treatment plants, or wetlands(Yacovitch et al., 2014). Carbon monoxide (CO) is produced during the incomplete combustion of any carbon-based fuel. Correlations between methane and ethane, and between methane and CO, can be used to differentiate among natural gas pre-meter leaks, post-combustion emissions, and microbial activities.

Previous studies have used both offline (Simpson et al., 2012; Schwietzke et al., 2025; Ren et al., 2018; Hopkins et al., 2016) and continuous (Karion et al., 2015; Yacovitch et al., 2017; Peischl et al., 2018; Maazallahi et al., 2020; Lamb et al., 2016; McKain et al., 2015; Plant et al., 2019; Floerchinger et al., 2021) observed ethane-to-methane enhancement (ΔC_2H_6:ΔCH_4) ratio relative to the composition of pipeline natural gas to quantify the fraction of thermogenic methane contributions, and used the correlations between CO and methane emissions to indicate the influences from combustion(Schiferl et al., 2025).

However, the reported natural gas composition across natural gas companies in NYCMA has large variations that lead to a great amount of uncertainty (Figure S4). Instead, we used high-resolution multi-trace gas correlations to identify natural gas plumes. The observed natural gas ethane-to-methane enhancement ratio provides a more accurate tracer:tracer relationship to quantify methane emissions from thermogenic sources than directly using reported pipeline numbers by natural gas companies.

When applying the tracer-tracer attribution approach, it is important to account for the dilution of the plume into ambient air (Brasseur and Jacob, 2017). The upwind natural gas plume mixes with background air with different ethane-to-methane ratios before reaching the measurement site can affect the linear correlations between co-emitted trace gases. In this study, we observed 0.03%–0.07% ethane-to-methane ratio in background air, compared to 1.9% to 4.6% ethane-to-methane ratio reported by local pipeline companies (Transco, Tetco, and Iroquois)(Williams Companies, 2025; Enbridge, 2025; Iroquois Gas Transmission System, LP., 2025). To minimize the influence of background dilution in this study, we account for non-clean background air effects by calculating the tracer-tracer ratio as the slope of linear correlations between trace gas enhancements (ΔCH_4:ΔC_2H_6, and ΔCH_4:ΔCO).

https://doi.org/10.5194/egusphere-2026-1742
Preprint. Discussion started: 11 May 2026

To identify thermogenic methane, we calculated the Reduced Major Axis (RMA) fit between 1 Hz ethane enhancements (ΔC_2H_6) and methane enhancements (ΔCH_4) for 5-minute tower measurement intervals, which considers variability in both x and y axes. To identify times of incomplete combustion, we calculated the fit between 1Hz CO enhancements (ΔCO) and ΔCH_4. Examples are shown in Figure 3. For each month with ethane observations, we defined the thermogenic methane plume as plumes with $R^2_{\Delta C_2H_6:\Delta CH_4} \geq 0.95$, and calculated the $R^2_{\Delta CO:\Delta CH_4}$ within those thermogenic plumes. We calculated the monthly thermogenic ΔC_2H_6:ΔCH_4 ratio as the slope using thermogenic 5-minute mean observations. We also calculated a mean monthly ΔC_2H_6:ΔCH_4 ratio as the slope using all 5-minute mean observations. The fraction of monthly methane emissions attributable to thermogenic sources was then obtained by dividing the mean observed ΔC_2H_6:ΔCH_4 ratio by the monthly thermogenic ratio (Figure S5).

2.6 Simulated methane enhancements

We calculated hourly simulated methane enhancements (ΔCH_4, ppb) by convolving a series of global, national, and regional methane emission inventories (units: nmol m^{-2} s^{-1}) with surface influence footprints (ppb (nmol m^{-2} s^{-1})$^{-1}$) derived from a Lagrangian atmospheric transport model:

$$\text{Simulated } \Delta CH_4 = \text{Inventory Emissions} \times \text{Surface-influence Footprint} \quad (2)$$

2.6.1 Methane Emission Inventories

We evaluated bottom-up methane emission estimates available at global, national and regional spatial scales (Table **??**). (i) At the **global** scale, we used the anthropogenic monthly 0.1 x 0.1° Emissions Database for Global Atmospheric Research (EDGAR) methane inventories v6.0 and v8.0 for 2018 and 2022 respectively; (ii) at the **national** scale, we analyzed the anthropogenic monthly 0.1 x 0.1° gridded Environmental Protection Agency (GEPA) inventory and the additional extended version (GEPA Extension) for the year 2018; (iii) at the **regional** scale, we used the annual 0.02 x 0.02° New York-Newark methane inventory by Pitt et al. (2024) (Pitt et al., 2024), which includes both anthropogenic and natural methane emissions for the New York-Newark area. For consistency, we subset the inventories to the same NYCMA domain and regridded the inventories to a 0.01° × 0.01° spatial resolution to match the surface influence footprint. Many studies have used the U.S. Census Bureau's Topologically Integrated Geographic Encoding and Referencing (TIGER) domain for New York area, which overlaps with most of NYCMA domain used in our study (Pitt et al., 2022, 2024; Nesser et al., 2024; Plant et al., 2019, 2022). Methane emission estimates in NYC from these analyses are thus comparable to results from this study.

(i) The EDGAR methane inventories provide global gridded methane emissions using international activity data and the Intergovernmental Panel on Climate Change source sectoral methodology(Crippa et al., 2020; European Commission. Joint Research Centre., 2023; Crippa et al., 2024). Methane emission estimates in EDGAR v6.0 ended in 2018, while EDGAR v8.0 extended activity data through 2022 and updated the residential activity data based on both population density and heating demand (Crippa et al., 2024, 2020). These updates resulted in total methane emissions in EDGAR v8.0 (2022) that were 14.6% lower than those in EDGAR v6.0 (2018) for NYCMA domain. The GEPA and EDGAR v6.0 methane inventories exhibited

https://doi.org/10.5194/egusphere-2026-1742
Preprint. Discussion started: 11 May 2026

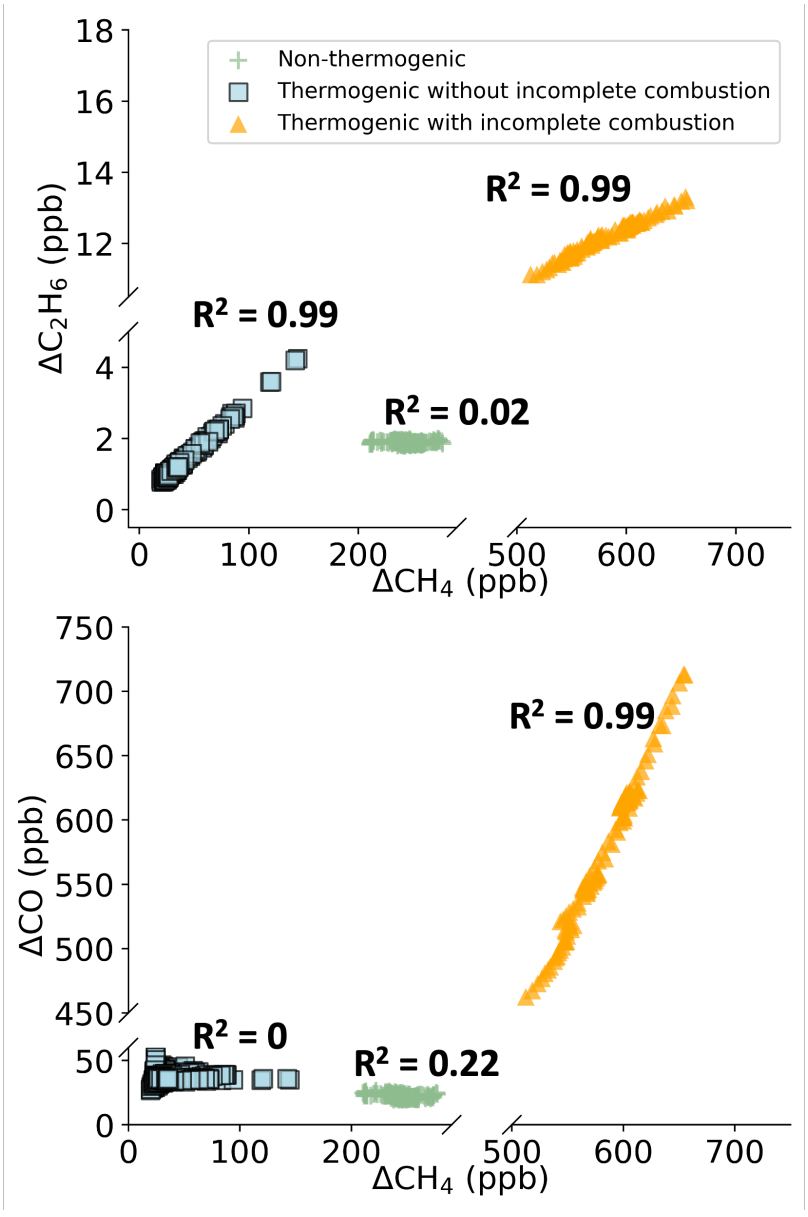

Figure 3. Examples of 1 Hz ΔC_2H_6:ΔCH_4 and ΔCO:ΔCH_4 from different source types observed over summer 2023 and February 2024. Natural gas-dominated plumes related to pre-meter leaks, such as during the distribution process with $R^2_{\Delta C_2H_6:\Delta CH_4} \geq 0.99$ & $R^2_{\Delta CO:\Delta CH_4} \leq 0.1$ (blue squares, observed on February 13^{th} 2024), natural gas-dominated plumes related to incomplete combustion activities, such as methane from incomplete combustion of natural gas from residential chimneys with $R^2_{\Delta C_2H_6:\Delta CH_4} \geq 0.99$ & $R^2_{\Delta CO:\Delta CH_4} \geq 0.99$ (orange triangles, observed on February 11^{th} 2024), and microbial activity-dominated plumes (often called non-thermogenic sectors) such as landfill, wastewater treatment plants, or natural wetlands with $R^2_{\Delta C_2H_6:\Delta CH_4} \leq 0.1$ (green crosses, observed on July 3^{rd} 2024).

https://doi.org/10.5194/egusphere-2026-1742
Preprint. Discussion started: 11 May 2026

similar total methane emissions for 2018 but displayed a low spatial correlation due to EDGAR allocating several large methane point sources to incorrect grid boxes (Figure S6) (Maasakkers et al., 2023).

(ii) GEPA methane inventories allocate sector-specific national anthropogenic methane emissions from the Inventory of U.S. Greenhouse Gas Emissions and Sinks (GHGI) to gridded emissions using proxy datasets (Maasakkers et al., 2023). The extended GEPA methane inventory includes additional emissions from the natural gas end-use sector (post-meter natural gas), primarily allocated based on post-meter activities from the Energy Information Administration (EIA) (Maasakkers et al., 2023). In NYCMA, revised estimates of natural gas emissions in the extended GEPA inventory for 2018 are 65% (±14.5%) larger than those in the main GEPA inventory, with additional post-meter sources accounting for more than 70% of this increase.

(iii) Pitt et al. (2024) (Pitt et al., 2024) developed high-resolution (0.02 x 0.02°) methane inventories for the New York-Newark domain (39.2°N, 42.0°N, 75.7°W, 72.1°W) for 2019, which account for both anthropogenic and natural methane emissions, including post-meter natural gas emissions. Methane emissions from Pitt et al. (2024) are about 1.3 times greater than the 2016 GEPA inventory in the NY-Newark urban area, which is defined using the U.S. Census Bureau's TIGER domain for New York. However, despite these updates, the methane emission fluxes remain a factor of 2.3 lower than estimates based on airborne observations(Pitt et al., 2024, 2022; Maasakkers et al., 2016). Pitt et al. (2024) developed an ensemble of 144 high-resolution methane flux maps by varying spatial distributions and emission factor proxies(Pitt et al., 2024). We selected 32 out of 144 versions of the Pitt et al. (2024) inventory based on higher mean and median correlation coefficients (R^2) between inventory estimates and airborne observations, as reported by Pitt et al. (2024)(Pitt et al., 2024). The Pitt et al. (2024) inventory applied in this study was calculated as the mean of these selected versions (Pitt et al., 2024).

2.6.2 Non-thermogenic Methane Sources in NYCMA

The dominant non-thermogenic methane sources are microbial in origin and include coastal wetlands, wastewater treatment plants, and landfills. The coastal wetlands in NYCMA are brackish with a seasonal cycle that is expected to peak in summer (Oikawa et al., 2024). Methane emissions from wastewater treatment plants are included in the local methane inventory for NYCMA, but the total number is poorly constrained (Pitt et al., 2024). There are no active landfills in the five boroughs of New York City, and only two active landfills in northern New Jersey within the 75% surface influence footprints for the Mineola Tower. These landfill methane emissions are included in the inventories, and together are about 1% of the total methane emissions estimated for February 2024 (EPA, 2024). Previous studies have pointed out that methane emissions from landfills may be higher in winter (Gillespie et al., 2024) and should be reassessed in the inventories. Our results show the microbial sources are unlikely to dominate methane emissions from the NYCMA.

2.6.3 Atmospheric Transport Model

The Lagrangian transport model applied in this study simulates hourly footprints, representing the surface influence on the air parcel at the specific moment when the observation is conducted. We used the Stochastic Time-Inverted Lagrangian Transport (STILT) Model to calculate the surface influence footprints. STILT is a Lagrangian particle dispersion model built on the Hybrid Single-Particle Lagrangian Integrated Trajectory (HYSPLIT) system with a distinct turbulent scheme (Fasoli et al.,

https://doi.org/10.5194/egusphere-2026-1742
Preprint. Discussion started: 11 May 2026

2018; Lin et al., 2003). STILT calculates sub-grid surface influence footprints from upstream areas in the planetary boundary layer (PBL) by tracing air particles backward in time with the meteorological field at a given location and height. Surface influence footprints quantify how surface emissions contribute to atmospheric trace gas dry mole fractions (Fasoli et al., 2018; Lin et al., 2003). In this study, we coupled STILT with 3 km High-Resolution Rapid Refresh (HRRR) meteorological fields (Benjamin et al., 2016)) and configured HRRR-STILT to trace 1000 air particles back 24 hours from the Mineola tower site to generate hourly 0.01 x 0.01° surface influence footprints from January 2023 to December 2024. Monthly-mean footprints at Mineola Tower 62 m AGL are shown in Figure S7.

2.6.4 Uncertainty Assessment

It is difficult to directly quantify the uncertainties in the surface influence footprint calculated by the Lagrangian transport model. Instead, we conducted a sensitivity study using alternative configurations of the atmospheric transport model and convolved the resulting surface influence footprints with inventories to simulate a range of methane enhancements (Eqn 2). None of the inventories used in this analysis have sub-monthly methane emission variations, so that all of the diel-scale changes in simulated ΔCH_4 are driven by meteorological variation in HRRR-STILT. Schiferl et al. (2025) (Schiferl et al., 2025) found that some configurations in HRRR-STILT altered the simulated methane enhancements more than others, especially the value of the minimum mixing layer height (MMLH). HRRR-STILT can calculate the mixed layer height in four ways: (1) sampled directly from the HRRR meteorological model outputs, (2) calculated from the temperature profile, (3) estimated using the turbulence kinetic energy, and (4) computed from the modified Richardson number (default). We evaluated the variability of the surface influence footprint calculated using these different configurations for May to August 2023. We also conducted sensitivity tests using different minimum mixed layer heights of 150 m and 250 m. We found that the choice of method to calculate mixed-layer height and the value of minimum mixed-layer height makes less than 1 ppb difference in the simulated methane enhancements during the afternoon when the boundary layer is high and well-mixed (Figure S8 & Figure S9). We also found that the simulated diel variability of ΔCH_4 closely matches the observed diel pattern, indicating that the Lagrangian transport model HRRR-STILT captured the overall atmospheric dynamics for the NYCMA (Figure S10). We adopted the default Richardson Number method to calculate the mixed-layer height with the default 150 m minimum height. We used only afternoon observations (12:00 to 18:00 local time), when HRRR–STILT simulations are least sensitive to model configuration choices, to quantify monthly methane emissions from the NYCMA.

We compared the monthly mean diel cycle of the observed and simulated ΔCH_4. The best agreement between observed and simulated ΔCH_4 was observed in May, especially in the afternoon (gray shading). Among the inventories, Pitt et al. (2024) consistently demonstrated the closest match to the observations and smallest underestimation of ΔCH_4, while EDGAR had the largest underestimate in almost every month. This discrepancy with EDGAR may reflect known issues with spatial allocation errors for large point sources in the Northeast U.S. region (Figure S6).

https://doi.org/10.5194/egusphere-2026-1742
Preprint. Discussion started: 11 May 2026

2.7 Observation-informed Methane Emissions

We calculated observation-informed methane emissions by applying a simulated scaling factor (SF) to the observed inventory. The SF allows us to capture biases in inventory methane emission fluxes while minimizing the impact of meteorological variability, and is widely applied in other studies over urban areas (Schiferl et al., 2025, 2024; Sargent et al., 2021). The simulated SF normalizes the observed methane enhancements by the simulated enhancements (Equation 3):

$$\text{Simulated SF} = \frac{\Delta\text{Observed CH}_4}{\Delta\text{Simulated CH}_4} \tag{3}$$

A simulated SF greater than one indicates that methane emissions are underestimated by the inventory, while a value less than one suggests that the inventory overestimates methane emissions. In this study, we calculated the afternoon SF for each month by applying 10000 bootstrapping draws with replacement for paired $\frac{\Delta\text{Observed CH}_4}{\Delta\text{Simulated CH}_4}$ with background variation. The SF calculations require at least 80 afternoon hours of valid paired observed and simulated ΔCH_4 for each month.

We then calculated the observation-informed methane emissions for each month (Equation 4) using

$$\text{Observation-informed Emission Flux} = \text{Inventory Emissions} \times \text{Simulated SF} \tag{4}$$

We quantified monthly observation-informed methane emissions for the afternoon only (12:00 to 18:00 EDT) and calculated the mean and 95% CI for each month by bootstrapping from the hourly observation-informed methane emission fluxes derived from all inventories during the afternoon (12 - 18 h), The 95% CI accounts for uncertainties in the ensemble of various methane inventories, background calculations, and variations in hourly observed and simulated ΔCH_4.

2.8 Methane Loss from Natural Gas Sectors

Previous studies have typically compared natural gas consumption with methane emissions using linear regression to quantify the natural gas methane loss rate in urban areas. This has been done either by (a) comparing natural gas methane consumptions with total estimated methane emissions(Karion et al., 2023b; Zeng et al., 2023; He et al., 2019), or (b) comparing natural gas methane consumptions with only the thermogenic portion of total methane emissions(Sargent et al., 2021; McKain et al., 2015). In this study, we explored both methods by calculating two cases of methane loss rates using different sets of estimated methane emissions: (1) observation-informed total methane emissions and (2) observed ΔC_2H_6:ΔCH_4 ratio inferred thermogenic methane emissions.

We used county-resolved natural gas deliveries to NYC (New York, Kings, Queens, Bronx, and Richmond counties)(S&P Global, 2025b) and northeast New Jersey (NE NJ; Bergen, Hudson, Passaic, Essex, Union, Middlesex, and Monmouth counties)(S&P Global, 2025a). The total methane delivered from the natural gas sector was calculated by multiplying monthly natural gas deliveries by the corresponding mean monthly natural gas methane percentage reported across three pipeline companies operating in NYCMA: Transco, Tetco, and Iroquois (assuming standard conditions of 60°F and 14.7 psia) (Williams Companies, 2025; Enbridge, 2025; Iroquois Gas Transmission System, LP., 2025).

We calculated the slope of the RMA linear regression to compare monthly observation-informed methane emissions with monthly natural gas methane delivered to NYC and NE NJ using two methods:

https://doi.org/10.5194/egusphere-2026-1742
Preprint. Discussion started: 11 May 2026

(1) We applied MODEL II RMA regression in R (gives the mean linear fit and 95% CI) to total monthly observation-based methane emissions and the total natural gas methane delivered to the NYCMA and northeast NJ for all months in 2023 and 2024. Here, we added NYCMA city core observation-based wintertime methane emissions from Schiferl et al., (2025)(Schiferl et al., 2025) for additional long-term constraints, but the inclusion of this data does not change any results.

(2) Adapting the methodologies of Sargent et al. (2012)(Sargent et al., 2021), and McKain et al. (2015)(McKain et al., 2015), we estimated observation-based natural gas methane emissions by scaling total methane emissions by the thermogenic fraction calculated as the ratio of monthly observed ΔC_2H_6:ΔCH_4 ratios to the monthly ΔC_2H_6:ΔCH_4 ratios of thermogenic plumes ($R^2_{\Delta C_2H_6:\Delta CH_4} \geq 0.95$). We applied a MODEL II RMA linear regression to the observation-based natural gas methane emissions and the total natural gas methane delivered to NYC and northeast NJ.

3 Results

We observed a strong seasonal cycle in observation-informed monthly methane emissions from January 2023 to December 2024, with peaks in months with winter heating and summer cooling loads. We found that thermogenic methane is the dominant source in both seasons, and the incomplete combustion of natural gas was the major signal observed. From the thermogenic methane emissions and delivered natural gas methane rates, we calculated a methane loss rate that is not included in the national methane inventory.

3.1 Observation-informed Methane Emission Rates

We identified distinct seasonal variations in methane emissions from NYCMA from January 2023 to December 2024 (Figure 4). The observation-informed emissions were high in winter months with building heating loads (in January and February), decreased from March to a minimum in May (two-year average of 6.3 $\pm$ 4.3 kg s^{-1}), and increased again in months with building cooling loads (June, July and August). Methane emissions increased further in the following heating season, with yearly maxima in November 2023 (15.9 $\pm$ 4.4 kg s^{-1}) and October 2024 (17.5 $\pm$ 4.8 kg s^{-1}), Monthly observation-informed methane emissions with 95% CI can be found in Table S3.

The seasonal cycle of methane emissions quantified for the suburban outflow is consistent with the city core methane emissions from Schiferl et al. (2025), which saw peak methane emissions in January and February, followed by a decline into spring(Schiferl et al., 2025). In general, the suburban observation-informed methane emissions in the spring months are slightly lower than the city core estimates, except in February 2023. The largest disagreement occurred in March of 2023, likely driven by reduced sampling at the urban core site, where they captured a high-emission period at the end of the month (Figure S11).

We observed a more pronounced seasonal cycle at the Mineola Tower compared with previous airborne-based methane emission estimates from before 2020. During the wintertime, we observed higher methane emissions (two-year averages of 13.2$\pm$8 kg s^{-1} in November, February, and March) than airborne-based estimates in the same month from 2018-2020 (9.7 $\pm$ 4.4 kg s^{-1} (Pitt et al., 2022)). But we observed lower methane emissions during the warmer months of April (2023: 9.0$\pm$4.7

https://doi.org/10.5194/egusphere-2026-1742
Preprint. Discussion started: 11 May 2026

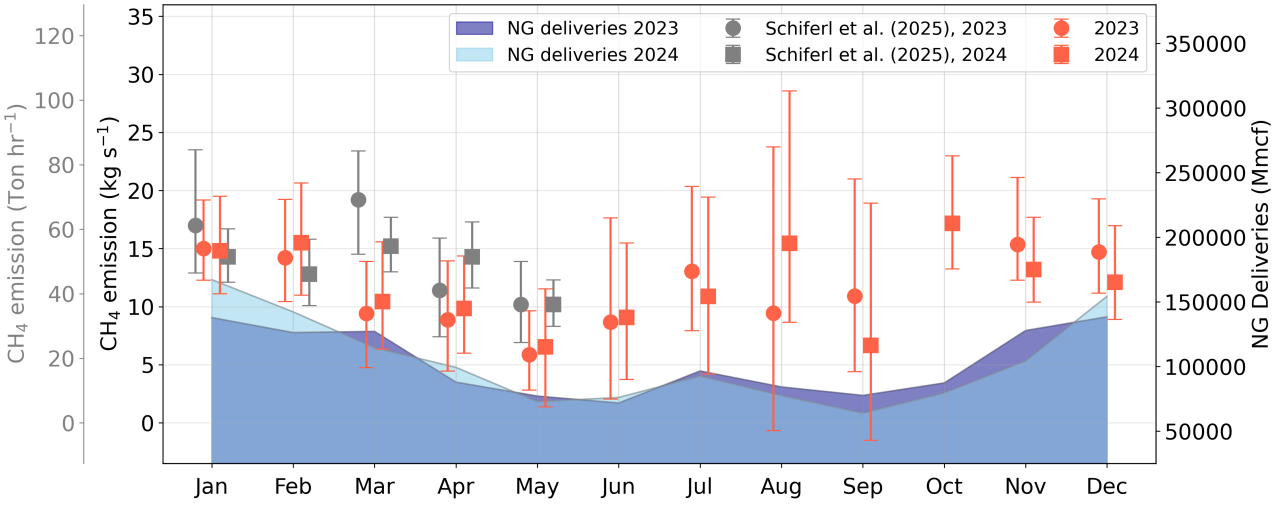

Figure 4. Observation-informed mean monthly methane emission rates from January to December in 2023 (red circles with 95% CI error bars) and 2024 (red squares, 95% CI error bars) for the NYCMA. Monthly observation-informed wintertime methane emissions from Schiferl et al. (2025) for NYCMA urban core are shown in grey (2023 in circles, and 2024 in squares)(Schiferl et al., 2025). Total natural gas deliveries to the NYCMA (in units of MMcf, Million cubic feet) are indicated in dark blue shading for 2023, and light blue shading for 2024.

and 2024: 9.9±4.1 kg s^{-1}) and May (2023: 6.0±3.4 and 2024: 6.5±5.1 kg s^{-1}) than estimated from aircraft in April 2018 (14.3±8.6 kg s^{-1}, (Plant et al., 2019)).

3.2 Methane Emissions from Thermogenic Sources

We observed that thermogenic sources dominated NYCMA methane emissions in the summer cooling and winter heating season. Thermogenic sources accounted for nearly all methane emissions in months with building heating loads (February and May; 98% thermogenic), whereas in months with building cooling loads (June, July, and August) there was a 12 to 15% non-thermogenic contribution. Tower observation-based thermogenic fractions are higher than previous studies using short-term airborne measurements. Among thermogenic plumes, incomplete combustion of natural gas was the major signal observed.

Thermogenic sources were dominant during both the summer cooling and winter heating season, and previous widely-applied approaches relying solely on fixed pipeline compositions tend to underestimate the thermogenic methane contribution in urban regions. As shown in Figure 5 (a), the estimated thermogenic methane fraction using this method was 88 ± 7% in June, 85 ± 11% in July, and 85 ± 12% in August. In the NYCMA heating season, we estimated thermogenic methane fractions of 99± 4% in February and 98 ± 9% in May. Floerchinger et al. (2021) calculated a thermogenic fraction of 81.5% (+0.4%, -0.6%) for New York City during the summer months using airborne observations and the local pipeline ethane-to-methane ratio(Floerchinger et al., 2021). Plant et al. (2019) estimated a thermogenic methane contribution of 87 ± 10% in winter using the airborne ethane-to-methane ratio compared with the Transco pipeline(Plant et al., 2019). These source attribution estimates fall within, but at the lower end of, our seasonal range.

https://doi.org/10.5194/egusphere-2026-1742
Preprint. Discussion started: 11 May 2026

Incomplete combustion of thermogenic sources is the dominant signal observed at Mineola Tower. We analyzed high-frequency (1 Hz) RMA correlations between ΔCO and ΔCH_4 within each 5-minute interval with $R^2_{\Delta C_2H_6:\Delta CH_4} \geq 0.95$, which represent thermogenic plumes with limited atmospheric mixing. A larger fraction of these thermogenic plumes exhibit high $R^2_{\Delta CO:\Delta CH_4}$ (Figure 5(b)). The majority of $R^2_{\Delta CO:\Delta CH_4}$ values exceed 0.7 during months with building heating demand and exceed 0.9 during months with building cooling demand. Thermogenic plumes with moderate $R^2_{\Delta CO:\Delta CH_4}$ (between 0.1 and 0.8) are observed more frequently during months with building heating loads (Figure S12), suggesting greater variability in combustion efficiency, likely driven by various natural gas combustion processes for heating purposes. These consistently high 1 Hz ΔCO:ΔCH_4 correlations across seasons demonstrate that incomplete combustion of natural gas is the dominant thermogenic methane process during both building heating and building cooling seasons. In contrast, only 7% (summer) and 6% (winter) of the identified thermogenic plumes were observed to have no combustion signature ($R^2_{\Delta CO:\Delta CH_4} < 0.1$), showing that natural gas emissions from pipeline leaks were less frequently observed at the Mineola tower compared to combustion-related natural gas sources. Similarly, Schiferl et al. (2025) identified incomplete combustion activities as a major contributor to wintertime methane emissions over NYCMA(Schiferl et al., 2025) using six years of observations. And the thermogenic methane emission driven by incomplete combustion of natural gas is a plausible explanation for why cities such as Boston have shown little to no decrease in methane emissions despite extensive efforts to repair natural gas pipeline leaks(Sargent et al., 2021).

3.3 Methane Loss Rate

There were strong positive linear relationships between observation-based thermogenic methane emissions and natural gas methane deliveries (R^2 = 0.90) (Figure 6). This pattern is consistent with thermogenic methane emissions that are primarily driven by post-meter end-use in the natural gas sector. These thermogenic emissions are proportional to natural gas consumption, while emissions from the local distribution system, which operates under relatively constant pipeline pressure, may remain stable throughout the year. The consumption-driven natural gas methane loss rate inferred from observed thermogenic ΔC_2H_6:ΔCH_4 ratios is 1.7±0.6% (95% CI), which is more than three times higher than the natural gas loss rate of 0.5% applied in the most recent bottom-up methane inventory for the NYCMA (Pitt et al., 2024). Comparing total methane emissions with delivered natural gas methane yielded a weaker correlation (R^2 = 0.28) and an estimated loss rate of 1.3±0.7% (Figure S13). The lower agreement likely reflects additional contributions from microbial sources such as wetlands during warmer months, a pattern also observed in Boston(Sargent et al., 2021). However, even when using total methane emissions, the inferred methane loss rate remains nearly 2.5 times higher than bottom-up estimates in the NYCMA (Pitt et al., 2024).

4 Conclusion and Discussion

We identified a distinct seasonal cycle in methane emissions across the NYCMA for 2023 and 2024. Observation-informed methane emissions peaked during the months with building heating (winter) and cooling (summer) loads, and declined steadily in the shoulder seasons. This temporal pattern correlates with peaks in natural gas deliveries for both winter heating and summer

https://doi.org/10.5194/egusphere-2026-1742
Preprint. Discussion started: 11 May 2026

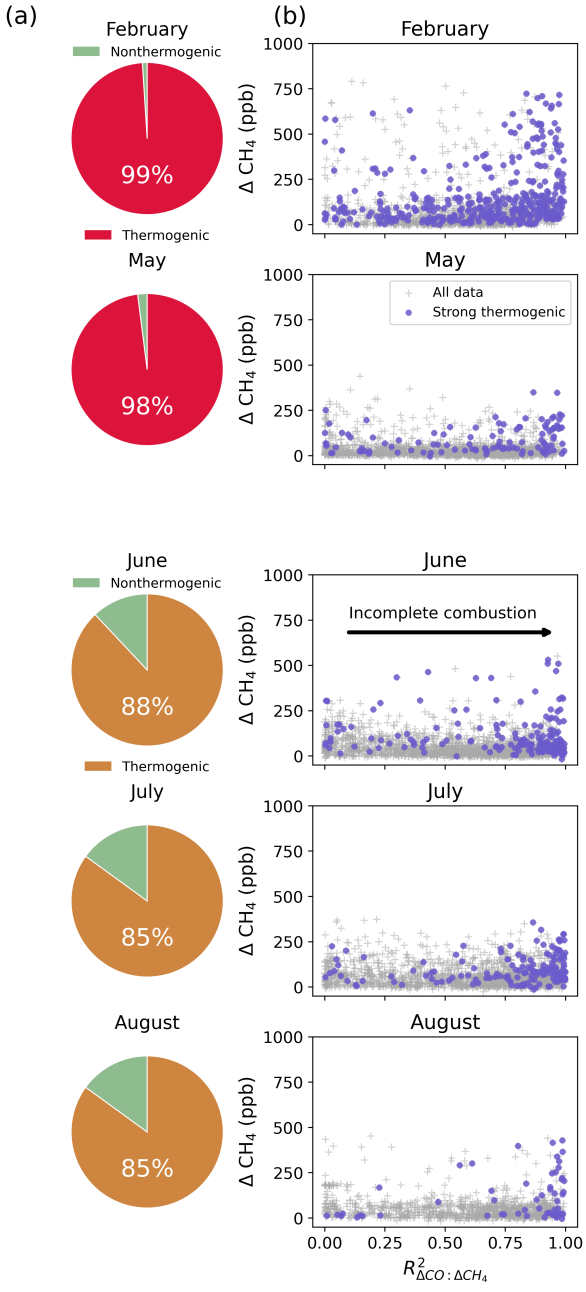

Figure 5. Monthly thermogenic fraction of total methane emissions and monthly incomplete combustion of natural gas signals. (a) Monthly thermogenic (red for heating season and orange for cooling months) and non-thermogenic (green) fractions of methane emissions. (b) Plot of 5-minute average ΔCH_4 as a function of the correlations between 1 Hz ΔCO and ΔCH_4 within each 5-minute interval for thermogenic plumes ($R^2_{\Delta C_2H_6:\Delta CH_4} \geq 0.95$, purple circle) and all 5-minute interval observations (gray cross).

https://doi.org/10.5194/egusphere-2026-1742
Preprint. Discussion started: 11 May 2026

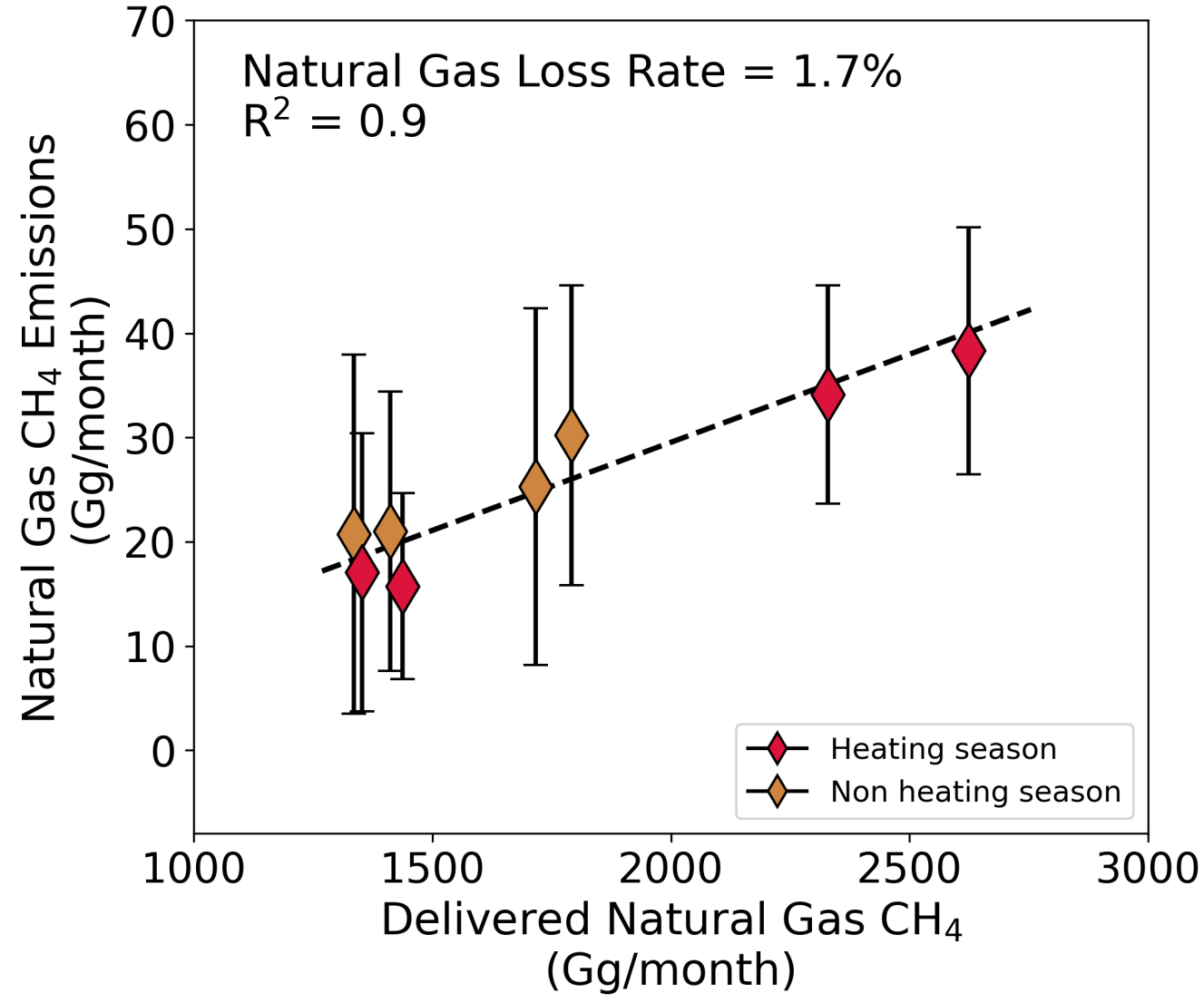

Figure 6. Observation-based natural gas methane emissions compared to natural gas methane delivered to NYC and northeast NJ for natural gas methane emissions using the observed ΔC_2H_6:ΔCH_4 ratio for heating (red diamonds; February, May) and non-heating (orange diamonds; June, July).

https://doi.org/10.5194/egusphere-2026-1742
Preprint. Discussion started: 11 May 2026

cooling seasons. With global temperatures continuing to rise, leading to more frequent, prolonged, and intense extreme weather events, including extreme heat and extended cold periods, energy demand for both cooling and heating is expected to grow. Without a transition to cleaner energy sources, this increased energy demand could lead to higher methane emissions in urban regions.

Source attribution analysis reveals that the incomplete combustion of natural gas (post-meter emissions from the inefficient burning of natural gas in any appliance or power unit) dominates methane emissions in the city, regardless of season. There is no natural gas methane loss rate currently included in national or global inventories (Crippa et al., 2024; Maasakkers et al., 2023), but the local NYCMA inventory(Pitt et al., 2024) has included a beyond-the-meter loss rate of 0.5% (Fischer et al., 2018). However, we calculated a consumption-driven loss rate for the NYCMA that is a factor of three times greater than these previous studies of appliance emissions. These largely overlooked combustion-related post-meter methane emissions can help explain the persistent missing thermogenic methane sources reported by previous studies.

The observed loss rate of 1.7±0.6% is within the range observed for other cities. It is less than the 2.5±0.5% (Sargent et al., 2021) and 2.7±0.6% (McKain et al., 2015) reported for the Boston area, but greater than the lower limit of the 1.3-2.3% reported for Los Angeles(He et al., 2019; Sargent et al., 2021) and the 1.3% reported for the Baltimore/DC area (Huang et al., 2019).

Many cities, including Boston, have dedicated millions of dollars to upgrading street-level natural gas infrastructure, without seeing any substantial change in methane emissions (Sargent et al., 2021). At the monthly retail prices of natural gas for 2023 and 2024, a 1.7% loss rate is close to 300 million USD per year of natural gas purchased, but unused, by consumers in New York City alone.

Our results highlight the three dimensional nature of urban methane emissions: the largest methane emissions are observed from rooftops and not from the pipelines beneath the streets below. Our findings emphasize the urgent need to incorporate emissions from post-meter natural gas combustion into methane inventories and emphasize emissions reductions from natural gas end-use sectors as a means to reduce urban methane emissions.

Data availability. Dryad link for peer-review only:
http://datadryad.org/share/LINK_NOT_FOR_PUBLICATION/uFWNB3b1t8cTmoSfLOvEkkJEYfWtUr7DNr7PV7ZwdsY

Author contributions. YZ and RC designed the study; YZ, AHD, TAM, MPV, DBM, DKF and RC conducted the fieldwork; YZ analyzed data with contributions from AHD and LDS; and YZ wrote the paper with RC and contributions from all co-authors.

Competing interests. There are no competing interests to declare.

https://doi.org/10.5194/egusphere-2026-1742
Preprint. Discussion started: 11 May 2026

Acknowledgements. The authors thank Anna Karion (NIST) and Lee Murray (University of Rochester) for data sharing. We also thank William Davies (Communications Leasing Inc.), Andrew Miller (Columbia University), and the FROG-NY team (Adam De Groodt, Emily Franklin, Rachel O'Brien, Katelyn Rediger, Rose Rossell) for support.

https://doi.org/10.5194/egusphere-2026-1742
Preprint. Discussion started: 11 May 2026

References

Benjamin, S. G., Weygandt, S. S., Brown, J. M., Hu, M., Alexander, C. R., Smirnova, T. G., Olson, J. B., James, E. P., Dowell, D. C., Grell, G. A., Lin, H., Peckham, S. E., Smith, T. L., Moninger, W. R., Kenyon, J. S., and Manikin, G. S.: A North American Hourly Assimilation and Model Forecast Cycle: The Rapid Refresh, Monthly Weather Review, 144, 1669–1694, https://doi.org/10.1175/MWR-D-15-0242.1, 2016.

Brasseur, G. P. and Jacob, D. J.: Atmospheric Observations and Model Evaluation, p. 436–486, Cambridge University Press, 2017.

Commane, R., Hallward-Driemeier, A., and Murray, L. T.: Intercomparison of commercial analyzers for atmospheric ethane and methane observations, Atmospheric Measurement Techniques, 16, 1431–1441, https://doi.org/10.5194/amt-16-1431-2023, 2023.

Crippa, M., Solazzo, E., Huang, G., Guizzardi, D., Koffi, E., Muntean, M., Schieberle, C., Friedrich, R., and Janssens-Maenhout, G.: High resolution temporal profiles in the Emissions Database for Global Atmospheric Research, Sci Data, 7, 121, https://doi.org/10.1038/s41597-020-0462-2, 2020.

Crippa, M., Guizzardi, D., Pagani, F., Schiavina, M., Melchiorri, M., Pisoni, E., Graziosi, F., Muntean, M., Maes, J., Dijkstra, L., Van Damme, M., Clarisse, L., and Coheur, P.: Insights into the spatial distribution of global, national, and subnational greenhouse gas emissions in the Emissions Database for Global Atmospheric Research (EDGAR v8.0), Earth System Science Data, 16, 2811–2830, https://doi.org/10.5194/essd-16-2811-2024, 2024.

Enbridge: Enbridge Texas Eastern InfoPost, https://infopost.enbridge.com/infopost/TEHome.asp?Pipe=TE, accessed 2025-12-13, 2025.

EPA: Inventory of U.S. Greenhouse Gas Emissions and Sinks: 1990-2022, Tech. rep., U.S. Environmental Protection Agency, EPA 430R-24004, https://www.epa.gov/ghgemissions/inventory-us-greenhouse-gas-emissions-and-sinks-1990-2022, 2024.

European Commission. Joint Research Centre.: GHG emissions of all world countries: 2023., Publications Office, LU, https://data.europa.eu/doi/10.2760/953322, 2023.

Fasoli, B., Lin, J. C., Bowling, D. R., Mitchell, L., and Mendoza, D.: Simulating atmospheric tracer concentrations for spatially distributed receptors: updates to the Stochastic Time-Inverted Lagrangian Transport model's R interface (STILT-R version 2), Geoscientific Model Development, 11, 2813–2824, https://doi.org/10.5194/gmd-11-2813-2018, 2018.

Fischer, M. L., Chan, W. R., Delp, W., Jeong, S., Rapp, V., and Zhu, Z.: An Estimate of Natural Gas Methane Emissions from California Homes, Environmental Science & Technology, 52, 10 205–10 213, https://doi.org/10.1021/acs.est.8b03217, pMID: 30071722, 2018.

Floerchinger, C., Shepson, P. B., Hajny, K., Daube, B. C., Stirm, B. H., Sweeney, C., and Wofsy, S. C.: Relative flux measurements of biogenic and natural gas-derived methane for seven U.S. cities, Elementa: Science of the Anthropocene, 9, 000 119, https://doi.org/10.1525/elementa.2021.000119, 2021.

Forster, P., Storelvmo, T., Armour, K., Collins, W., Dufresne, J.-L., Frame, D., Lunt, D. J., Mauritsen, T., Palmer, M. D., Watanabe, M., Wild, M., and Zhang, X.: The Earth's energy budget, climate feedbacks, and climate sensitivity, in: Climate Change 2021: The Physical Science Basis. Contribution of Working Group I to the Sixth Assessment Report of the Intergovernmental Panel on Climate Change, edited by Masson-Delmotte, V., Zhai, P., Pirani, A., Connors, S. L., Péan, C., Berger, S., Caud, N., Chen, Y., Goldfarb, L., Gomis, M. I., Huang, M., Leitzell, K., Lonnoy, E., Matthews, J. B. R., Maycock, T. K., Waterfield, T., Yelekçi, Ö., Yu, R., and Zhou, B., pp. 923–1054, Cambridge University Press, Cambridge, United Kingdom and New York, NY, USA, https://doi.org/10.1017/9781009157896.001, 2021.

Gillespie, L. D., Ars, S., Alkadri, S., Urya, S., Khoo, T., Fraser, S., Vogel, F., and Wunch, D.: Estimating methane emissions from the waste sector in southern ontario using atmospheric measurements, Journal of the Air & Waste Management Association, p. 10962247.2024.2435340, https://doi.org/10.1080/10962247.2024.2435340, 2024.

https://doi.org/10.5194/egusphere-2026-1742
Preprint. Discussion started: 11 May 2026

Global Methane Pledge: www.globalmethanepledge.org, accessed: 2025-02-28, 2021.

He, L., Zeng, Z.-C., Pongetti, T. J., Wong, C., Liang, J., Gurney, K. R., Newman, S., Yadav, V., Verhulst, K., Miller, C. E., Duren, R., Frankenberg, C., Wennberg, P. O., Shia, R.-L., Yung, Y. L., and Sander, S. P.: Atmospheric Methane Emissions Correlate With Natural Gas Consumption From Residential and Commercial Sectors in Los Angeles, Geophysical Research Letters, 46, 8563–8571, https://doi.org/10.1029/2019GL083400, _eprint: https://agupubs.onlinelibrary.wiley.com/doi/pdf/10.1029/2019GL083400, 2019.

Hopkins, F. M., Kort, E. A., Bush, S. E., Ehleringer, J. R., Lai, C.-T., Blake, D. R., and Randerson, J. T.: Spatial patterns and source attribution of urban methane in the Los Angeles Basin, Journal of Geophysical Research: Atmospheres, 121, 2490–2507, https://doi.org/10.1002/2015JD024429, 2016.

Huang, Y., Kort, E. A., Gourdji, S., Karion, A., Mueller, K., and Ware, J.: Seasonally Resolved Excess Urban Methane Emissions from the Baltimore/Washington, DC Metropolitan Region, Environ. Sci. Technol., 53, 11 285–11 293, https://doi.org/10.1021/acs.est.9b02782, 2019.

Iroquois Gas Transmission System, LP.: Daily Gas Quality Reporting, https://ioly.iroquois.com/infopost/#dailygasqualityreport, accessed 2025-12-13, 2025.

Karion, A., Sweeney, C., Kort, E. A., Shepson, P. B., Brewer, A., Cambaliza, M., Conley, S. A., Davis, K., Deng, A., Hardesty, M., Herndon, S. C., Lauvaux, T., Lavoie, T., Lyon, D., Newberger, T., Pétron, G., Rella, C., Smith, M., Wolter, S., Yacovitch, T. I., and Tans, P.: Aircraft-Based Estimate of Total Methane Emissions from the Barnett Shale Region, Environmental Science & Technology, 49, 8124–8131, https://doi.org/10.1021/acs.est.5b00217, 2015.

Karion, A., Callahan, W., Stock, M., Prinzivalli, S., Verhulst, K. R., Kim, J., Salameh, P. K., Lopez-Coto, I., and Whetstone, J.: Greenhouse gas observations from the Northeast Corridor tower network, Earth System Science Data, 12, 699–717, https://doi.org/10.5194/essd-12-699-2020, 2020.

Karion, A., DiGangi, E., Prinzivalli, S., Draper, C., Baldelli, S., Fain, C., Biggs, B., Stock, M., Michalak, B., Salameh, P., Kim, J., Callahan, W., and Whetstone, J.: Observations of carbon dioxide (CO2), methane (CH4), and carbon monoxide (CO) mole fractions from the NIST Northeast Corridor urban testbed, https://doi.org/10.18434/MDS2-3012, 2023a.

Karion, A., Ghosh, S., Lopez-Coto, I., Mueller, K., Gourdji, S., Pitt, J., and Whetstone, J.: Methane Emissions Show Recent Decline but Strong Seasonality in Two US Northeastern Cities, Environmental Science & Technology, 57, 19 565–19 574, https://doi.org/10.1021/acs.est.3c05050, pMID: 37941355, 2023b.

Lamb, B. K., Cambaliza, M. O. L., Davis, K. J., Edburg, S. L., Ferrara, T. W., Floerchinger, C., Heimburger, A. M. F., Herndon, S., Lauvaux, T., Lavoie, T., Lyon, D. R., Miles, N., Prasad, K. R., Richardson, S., Roscioli, J. R., Salmon, O. E., Shepson, P. B., Stirm, B. H., and Whetstone, J.: Direct and Indirect Measurements and Modeling of Methane Emissions in Indianapolis, Indiana, Environmental Science & Technology, 50, 8910–8917, https://doi.org/10.1021/acs.est.6b01198, publisher: American Chemical Society, 2016.

Lebel, E. D., Finnegan, C. J., Ouyang, Z., and Jackson, R. B.: Methane and NOx Emissions from Natural Gas Stoves, Cooktops, and Ovens in Residential Homes, Environmental Science & Technology, 56, 2529–2539, https://doi.org/10.1021/acs.est.1c04707, pMID: 35081712, 2022.

Lin, J. C., Gerbig, C., Wofsy, S. C., Andrews, A. E., Daube, B. C., Davis, K. J., and Grainger, C. A.: A near-field tool for simulating the upstream influence of atmospheric observations: The Stochastic Time-Inverted Lagrangian Transport (STILT) model, Journal of Geophysical Research: Atmospheres, 108, https://doi.org/10.1029/2002JD003161, 2003.

Lopez, M., Sherwood, O., Dlugokencky, E., Kessler, R., Giroux, L., and Worthy, D.: Isotopic signatures of anthropogenic CH4 sources in Alberta, Canada, Atmospheric Environment, 164, 280–288, https://doi.org/10.1016/j.atmosenv.2017.06.021, 2017.

https://doi.org/10.5194/egusphere-2026-1742
Preprint. Discussion started: 11 May 2026

Maasakkers, J. D., Jacob, D. J., Sulprizio, M. P., Turner, A. J., Weitz, M., Wirth, T., Hight, C., DeFigueiredo, M., Desai, M., Schmeltz, R., Hockstad, L., Bloom, A. A., Bowman, K. W., Jeong, S., and Fischer, M. L.: Gridded National Inventory of U.S. Methane Emissions, Environ. Sci. Technol., 50, 13 123–13 133, https://doi.org/10.1021/acs.est.6b02878, 2016.

Maasakkers, J. D., McDuffie, E. E., Sulprizio, M. P., Chen, C., Schultz, M., Brunelle, L., Thrush, R., Steller, J., Sherry, C., Jacob, D. J., Jeong, S., Irving, B., and Weitz, M.: A Gridded Inventory of Annual 2012–2018 U.S. Anthropogenic Methane Emissions, Environ. Sci. Technol., 57, 16 276–16 288, https://doi.org/10.1021/acs.est.3c05138, 2023.

Maazallahi, H., Fernandez, J. M., Menoud, M., Zavala-Araiza, D., Weller, Z. D., Schwietzke, S., Von Fischer, J. C., Denier Van Der Gon, H., and Röckmann, T.: Methane mapping, emission quantification, and attribution in two European cities: Utrecht (NL) and Hamburg (DE), Atmospheric Chemistry and Physics, 20, 14 717–14 740, https://doi.org/10.5194/acp-20-14717-2020, 2020.

McKain, K., Down, A., Raciti, S. M., Budney, J., Hutyra, L. R., Floerchinger, C., Herndon, S. C., Nehrkorn, T., Zahniser, M. S., Jackson, R. B., Phillips, N., and Wofsy, S. C.: Methane emissions from natural gas infrastructure and use in the urban region of Boston, Massachusetts, Proceedings of the National Academy of Sciences, 112, 1941–1946, https://doi.org/10.1073/pnas.1416261112, 2015.

Menoud, M., Van Der Veen, C., Maazallahi, H., Hensen, A., Velzeboer, I., Van Den Bulk, P., Delre, A., Korben, P., Schwietzke, S., Ardelean, M., Calcan, A., Etiope, G., Baciu, C., Scheutz, C., Schmidt, M., and Röckmann, T.: CH4 isotopic signatures of emissions from oil and gas extraction sites in Romania, Elementa: Science of the Anthropocene, 10, 00 092, https://doi.org/10.1525/elementa.2021.00092, 2022.

Merrin, Z. and Francisco, P. W.: Unburned Methane Emissions from Residential Natural Gas Appliances, Environmental Science & Technology, 53, 5473–5482, https://doi.org/10.1021/acs.est.8b05323, 2019.

Mielke-Maday, I., Schwietzke, S., Yacovitch, T. I., Miller, B., Conley, S., Kofler, J., Handley, P., Thorley, E., Herndon, S. C., Hall, B., Dlugokencky, E., Lang, P., Wolter, S., Moglia, E., Crotwell, M., Crotwell, A., Rhodes, M., Kitzis, D., Vaughn, T., Bell, C., Zimmerle, D., Schnell, R., and Pétron, G.: Methane source attribution in a U.S. dry gas basin using spatial patterns of ground and airborne ethane and methane measurements, Elementa: Science of the Anthropocene, 7, 13, https://doi.org/10.1525/elementa.351, 2019.

Mueller, K. L., Karion, A., Lopez-Coto, I., Marrs, J., Yadav, V., Plant, G., Pitt, J., Barkley, Z. R., and Whetstone, J.: Scaling Urban Methane Emissions: Utility of Single-Site Measurements in Five Urban Domains, Environmental Science & Technology, 59, 14 399–14 409, https://doi.org/10.1021/acs.est.5c03844, pMID: 40633562, 2025.

Naik, V., Szopa, S., Adhikary, B., Artaxo Netto, P. E., Berntsen, T., Collins, W. D., Fuzzi, S., Gallardo, L., Kiendler-Scharr, A., Klimont, Z., Liao, H., Unger, N., and Zanis, P.: Short-lived climate forcers, in: Climate Change 2021: The Physical Science Basis. Contribution of Working Group I to the Sixth Assessment Report of the Intergovernmental Panel on Climate Change, edited by Masson-Delmotte, V., Zhai, P., Pirani, A., Connors, S. L., Péan, C., Berger, S., Caud, N., Chen, Y., Goldfarb, L., Gomis, M. I., Huang, M., Leitzell, K., Lonnoy, E., Matthews, J. B. R., Maycock, T. K., Waterfield, T., Yelekçi, Ö., Yu, R., and Zhou, B., pp. 817–922, Cambridge University Press, Cambridge, United Kingdom and New York, NY, USA, https://doi.org/10.1017/9781009157896.001, 2021.

Nesser, H., Jacob, D. J., Maasakkers, J. D., Lorente, A., Chen, Z., Lu, X., Shen, L., Qu, Z., Sulprizio, M. P., Winter, M., Ma, S., Bloom, A. A., Worden, J. R., Stavins, R. N., and Randles, C. A.: High-resolution US methane emissions inferred from an inversion of 2019 TROPOMI satellite data: contributions from individual states, urban areas, and landfills, Atmospheric Chemistry and Physics, 24, 5069–5091, https://doi.org/10.5194/acp-24-5069-2024, 2024.

New York City Housing Authority: Heating Season, https://www.nyc.gov/site/nycha/residents/heating.page, accessed 2025-11-30, 2025.

Oikawa, P. Y., Sihi, D., Forbrich, I., Fluet-Chouinard, E., Najarro, M., Thomas, O., Shahan, J., Arias-Ortiz, A., Russell, S., Knox, S. H., McNicol, G., Wolfe, J., Windham-Myers, L., Stuart-Haentjens, E., Bridgham, S. D., Needelman, B., Vargas, R., Schäfer, K., Ward, E. J., Megonigal, P., and Holmquist, J.: A New Coupled Biogeochemical Modeling Approach Provides Accurate Predictions of Methane

https://doi.org/10.5194/egusphere-2026-1742
Preprint. Discussion started: 11 May 2026

and Carbon Dioxide Fluxes Across Diverse Tidal Wetlands, Journal of Geophysical Research: Biogeosciences, 129, e2023JG007 943, https://doi.org/https://doi.org/10.1029/2023JG007943, e2023JG007943 2023JG007943, 2024.

Peischl, J., Eilerman, S. J., Neuman, J. A., Aikin, K. C., De Gouw, J., Gilman, J. B., Herndon, S. C., Nadkarni, R., Trainer, M., Warneke, C., and Ryerson, T. B.: Quantifying Methane and Ethane Emissions to the Atmosphere From Central and Western U.S. Oil and Natural Gas Production Regions, Journal of Geophysical Research: Atmospheres, 123, 7725–7740, https://doi.org/10.1029/2018JD028622, 2018.

Pitt, J. R., Lopez-Coto, I., Hajny, K. D., Tomlin, J., Kaeser, R., Jayarathne, T., Stirm, B. H., Floerchinger, C. R., Loughner, C. P., Gately, C. K., Hutyra, L. R., Gurney, K. R., Roest, G. S., Liang, J., Gourdji, S., Karion, A., Whetstone, J. R., and Shepson, P. B.: New York City greenhouse gas emissions estimated with inverse modeling of aircraft measurements, Elementa: Science of the Anthropocene, 10, 00 082, https://doi.org/10.1525/elementa.2021.00082, 2022.

Pitt, J. R., Lopez-Coto, I., Karion, A., Hajny, K. D., Tomlin, J., Kaeser, R., Jayarathne, T., Stirm, B. H., Floerchinger, C. R., Loughner, C. P., Commane, R., Gately, C. K., Hutyra, L. R., Gurney, K. R., Roest, G. S., Liang, J., Gourdji, S., Mueller, K. L., Whetstone, J. R., and Shepson, P. B.: Underestimation of Thermogenic Methane Emissions in New York City, Environ. Sci. Technol., 58, 9147–9157, https://doi.org/10.1021/acs.est.3c10307, 2024.

Plant, G., Kort, E. A., Floerchinger, C., A. Gvakharia, Gvakharia, A., Vimont, I., Vimont, I., and Sweeney, C.: Large Fugitive Methane Emissions From Urban Centers Along the U.S. East Coast., Geophysical Research Letters, 46, 8500–8507, https://doi.org/10.1029/2019gl082635, 2019.

Plant, G., Kort, E. A., Murray, L. T., Maasakkers, J. D., and Aben, I.: Evaluating urban methane emissions from space using TROPOMI methane and carbon monoxide observations, Remote Sensing of Environment, 268, 112 756, https://doi.org/10.1016/j.rse.2021.112756, 2022.

Ren, X., Salmon, O. E., Hansford, J. R., Ahn, D., Hall, D., Benish, S. E., Stratton, P. R., He, H., Sahu, S., Grimes, C., Heimburger, A. M. F., Martin, C. R., Cohen, M. D., Stunder, B., Salawitch, R. J., Ehrman, S. H., Shepson, P. B., and Dickerson, R. R.: Methane Emissions From the Baltimore-Washington Area Based on Airborne Observations: Comparison to Emissions Inventories, Journal of Geophysical Research: Atmospheres, 123, 8869–8882, https://doi.org/10.1029/2018JD028851, 2018.

Saint-Vincent, P. M. B. and Pekney, N. J.: Beyond-the-Meter: Unaccounted Sources of Methane Emissions in the Natural Gas Distribution Sector, Environmental Science & Technology, 54, 39–49, https://doi.org/10.1021/acs.est.9b04657, pMID: 31809030, 2020.

Sargent, M. R., Floerchinger, C., McKain, K., Budney, J., Gottlieb, E. W., Hutyra, L. R., Rudek, J., and Wofsy, S. C.: Majority of US urban natural gas emissions unaccounted for in inventories, Proceedings of the National Academy of Sciences, 118, e2105804 118, https://doi.org/10.1073/pnas.2105804118, 2021.

Schiavina, M., Melchiorri, M., and Pesaresi, M.: GHS-SMOD R2023A - GHS Settlement Layers, Application of the Degree of Urbanisation Methodology (Stage I) to GHS-POP R2023A and GHS-BUILT-S R2023A, Multitemporal (1975-2030), https://doi.org/10.2905/A0DF7A6F-49DE-46EA-9BDE-563437A6E2BA, 2023.

Schiferl, L. D., Cao, C., Dalton, B., Hallward-Driemeier, A., Toledo-Crow, R., and Commane, R.: Multi-year observations of variable incomplete combustion in the New York megacity, Atmospheric Chemistry and Physics, 24, 10 129–10 142, https://doi.org/10.5194/acp-24-10129-2024, 2024.

Schiferl, L. D., Hallward-Driemeier, A., Zhao, Y., Toledo-Crow, R., and Commane, R.: Missing wintertime methane emissions from New York City related to combustion, Atmospheric Chemistry and Physics, 25, 15 683–15 700, https://doi.org/10.5194/acp-25-15683-2025, 2025.

https://doi.org/10.5194/egusphere-2026-1742
Preprint. Discussion started: 11 May 2026

Schwietzke, S., Griffin, W. M., Matthews, H. S., and Bruhwiler, L. M. P.: Natural Gas Fugitive Emissions Rates Constrained by Global Atmospheric Methane and Ethane, Environmental Science & Technology, 48, 7714–7722, https://doi.org/10.1021/es501204c, 2025.

Shindell, D., Ravishankara, A. R., Kuylenstierna, J. C. I., Michalopoulou, E., Höglund-Isaksson, L., Zhang, Y., Seltzer, K., Ru, M., Castelino, R., Faluvegi, G., Naik, V., Horowitz, L., He, J., Lamarque, J.-F., Sudo, K., Collins, W. J., Malley, C., Harmsen, M., Stark, K., Junkin, J., Li, G., Glick, A., and Borgford-Parnell, N.: Global Methane Assessment: Benefits and Costs of Mitigating Methane Emissions, 2021.

Simpson, I. J., Sulbaek Andersen, M. P., Meinardi, S., Bruhwiler, L., Blake, N. J., Helmig, D., Rowland, F. S., and Blake, D. R.: Long-term decline of global atmospheric ethane concentrations and implications for methane, Nature, 488, 490–494, https://doi.org/10.1038/nature11342, 2012.

S&P Global: Connect. PointLogic. Select NJ Counties Distribution and Power, subscription Access on November 20, 2025, 2025a.

S&P Global: Connect. PointLogic. Select NY Counties Distribution and Power, subscription Access on November 20, 2025, 2025b.

Ueyama, M., Nakaoka, A., Umezawa, T., Terao, Y., and Lunt, M.: Natural Gas and Biogenic CH4 Emissions from an Urban Center, Sakai, Japan, Based on Simultaneous Measurements of CH4 and C2H6 fluxes Based on the Eddy Covariance Method, Environmental Science & Technology, 59, 25 877–25 888, https://doi.org/10.1021/acs.est.5c09629, pMID: 41298272, 2025.

United Nations Environment Programme: About International Methane Emissions Observatory (IMEO), https://www.unep.org/topics/energy/methane/about-imeo, accessed: 2026-01-13, 2025a.

United Nations Environment Programme: Methane Alert and Response System (MARS), https://www.unep.org/topics/energy/methane/methane-alert-and-response-system-mars, accessed: 2026-01-13, 2025b.

Vanselow, S., Schneising, O., Buchwitz, M., Reuter, M., Bovensmann, H., Boesch, H., and Burrows, J. P.: Automated detection of regions with persistently enhanced methane concentrations using Sentinel-5 Precursor satellite data, Atmospheric Chemistry and Physics, 24, 10 441–10 473, https://doi.org/10.5194/acp-24-10441-2024, 2024.

Verhulst, K. R., Karion, A., Kim, J., Salameh, P. K., Keeling, R. F., Newman, S., Miller, J., Sloop, C., Pongetti, T., Rao, P., Wong, C., Hopkins, F. M., Yadav, V., Weiss, R. F., Duren, R. M., and Miller, C. E.: Carbon dioxide and methane measurements from the Los Angeles Megacity Carbon Project – Part 1: calibration, urban enhancements, and uncertainty estimates, Atmospheric Chemistry and Physics, 17, 8313–8341, https://doi.org/10.5194/acp-17-8313-2017, 2017.

Welp, L. R., Keeling, R. F., Weiss, R. F., Paplawsky, W., and Heckman, S.: Design and performance of a Nafion dryer for continuous operation at CO_2 and CH_4 air monitoring sites, Atmospheric Measurement Techniques, 6, 1217–1226, https://doi.org/10.5194/amt-6-1217-2013, 2013.

Williams Companies: Transco Pipeline - 1Line System, https://www.1line.williams.com/Transco/index.html, accessed 2025-12-13, 2025.

Yacovitch, T. I., Herndon, S. C., Roscioli, J. R., Floerchinger, C., McGovern, R. M., Agnese, M., Pétron, G., Kofler, J., Sweeney, C., Karion, A., Conley, S. A., Kort, E. A., Nähle, L., Fischer, M., Hildebrandt, L., Koeth, J., McManus, J. B., Nelson, D. D., Zahniser, M. S., and Kolb, C. E.: Demonstration of an Ethane Spectrometer for Methane Source Identification, Environmental Science & Technology, 48, 8028–8034, https://doi.org/10.1021/es501475q, 2014.

Yacovitch, T. I., Daube, C., Vaughn, T. L., Bell, C. S., Roscioli, J. R., Knighton, W. B., Nelson, D. D., Zimmerle, D., Pétron, G., and Herndon, S. C.: Natural gas facility methane emissions: measurements by tracer flux ratio in two US natural gas producing basins, Elementa: Science of the Anthropocene, 5, 69, https://doi.org/10.1525/elementa.251, 2017.

Zeng, Z.-C., Pongetti, T., Newman, S., Oda, T., Gurney, K., Palmer, P. I., Yung, Y. L., and Sander, S. P.: Decadal decrease in Los Angeles methane emissions is much smaller than bottom-up estimates, Nature Communications, 14, 5353, https://doi.org/10.1038/s41467-023-40964-w, publisher: Nature Publishing Group, 2023.